Supplementary information for "Fast unconditional reset and leakage reduction in fixed-frequency transmon qubits"

Liangyu Chen[1*], Simon Pettersson Fors[1], Zixian Yan[1], Anaida Ali[1], Tahereh Abad[1], Amr Osman[1], Eleftherios Moschandreou[1], Benjamin Lienhard[2,3], Sandoko Kosen[1], Hang-Xi Li[1], Daryoush Shiri[1], Tong Liu[1], Stefan Hill[1], Abdullah-Al Amin[1], Robert Rehammar[1], Mamta Dahiya[1], Andreas Nylander[1], Marcus Rommel[1], Anita Fadavi Roudsari[1], Marco Caputo[4], Leif Grönberg [4], Joonas Govenius[4], Miroslav Dobsicek[1], Michele Faucci Giannelli[1], Anton Frisk Kockum[1], Jonas Bylander[1], Giovanna Tancredi[1,*]

[1]*Department of Microtechnology and Nanoscience, Chalmers University of Technology, 41296 Gothenburg, Sweden.*

[2]*Department of Chemistry, Princeton University, Princeton, NJ 08544, USA*

[3]*Department of Electrical and Computer Engineering, Princeton University, Princeton, NJ 08544, USA*

[4]*VTT Technical Research Centre of Finland, FI-02044 VTT, Finland*

Supplementary Note I : Experimental setup

The parameters of the sample used in our experiment are listed in Table S1. The device is installed in a Bluefors dilution refrigerator and cooled below 10 mK. The full wiring diagram is shown in Fig. S1. The drive pulses for the qubits are generated by a two-channel signal generator (*QBLOX Instruments* QCM-RF).

The readout pulse consists of a flat-top pulse with Gaussian rising and falling edges with a width of 10 ns, which is generated by a high-frequency lock-in amplifier (*QBLOX Instruments* QRM-RF) to match the corresponding readout frequency of the individual resonators. The transmitted readout signal through the sample is amplified by around 39 dB at 4 K with a high-electron-mobility transistor (HEMT, LNF-LNC4_8C) amplifier. Additionally, two amplifiers are connected to the readout chain outside of the dilution fridge. Finally, the output signal is down-converted to the hundreds of MHz range to be recorded and integrated by the QRM-RF.

The biased current for the coupler is supplied by a current source (*QBLOX Instruments* S4g) and the flux pulse is generated by a four-channel arbitrary waveform generator (*QBLOX Instruments* QCM) operating at baseband frequency. The DC and AC flux signal is coupled together with a bias tee at the 10mK stage.

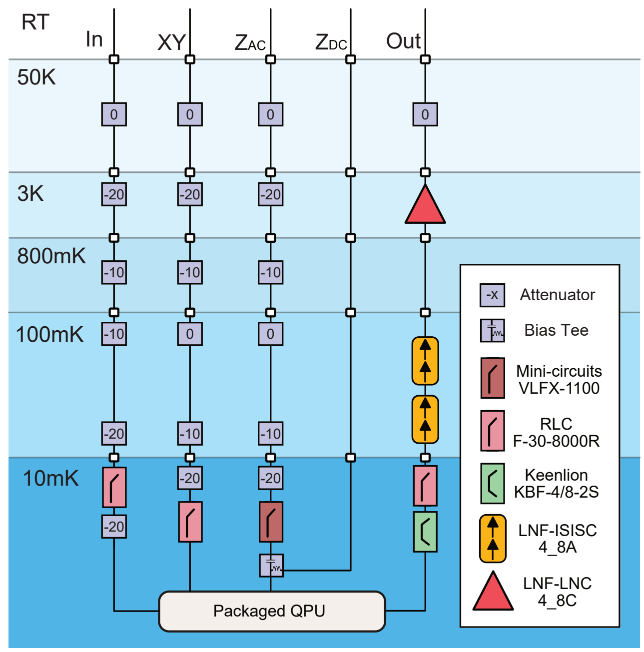

Figure S1. **Full wiring diagram for the experimental setup including the circuit model of the tested chip.** XY: qubit XY-drive line, Z_{DC}: coupler bias current line, Z_{AC}: coupler flux pulse line, RT: room temperature.

Supplementary Note II : Data qubit response

One limiting constraint on the adiabaticity of the reset pulse is the frequency spacing between the two qubits. In Fig. S2, two sets of measurements are carried out for the same reset pulse with Q_1 initially prepared in either $|0\rangle$ [Fig. S2(a-b)] or $|1\rangle$ [Fig. S2(c-d)]. We observe that the parameter space available for a complete reset for Q_0 in Fig. S2(a) is much larger than that in Fig. S2(c). The transition in this regime is fully adiabatic, indicated by the fact that there is no oscillation occurring at a longer pulse duration.

However, reset pulses with these parameters move the coupler too close to the Q_1 frequency, resulting in significant undesirable interaction with Q_1, as shown more prominently in Fig. S2(d). Therefore, in order to protect the $|1\rangle$-state population of Q_1, we choose to operate in the regime indicated by Fig. S2(c). This constraint increases the calibration difficulty and potentially decreases long-term stability in large devices.

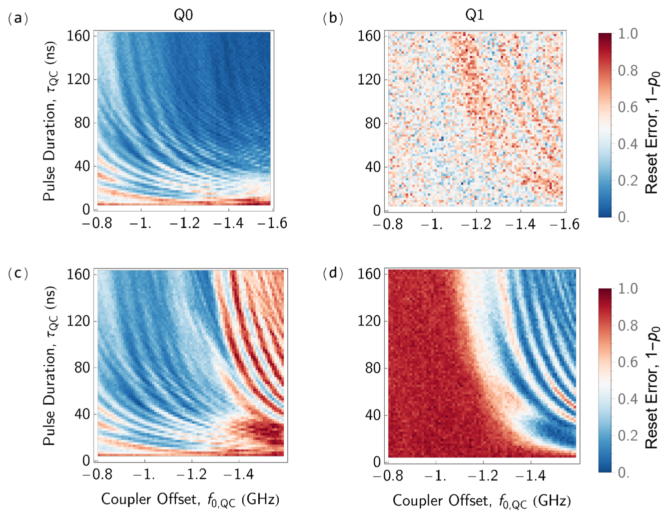

Figure S2. **Adiabatic pulse performance with respect to the excitation on the data qubit.** In **(a-b)** (**(c-d)**), Q_1 is initially prepared in $|0\rangle$ ($|1\rangle$)-state. The interaction between the coupler and Q_0 varies much differently depending on the state of Q_1. The coupling strength parameter g is set to 1 GHz for both measurements to approximate a linear ramp pulse.

Parameters		Q_0	Q_1
Qubit frequency	$\omega_q/2\pi$ (GHz)	5.176	4.534
Qubit anharmonicity	$\alpha/2\pi$ (MHz)	-256	-158
Resonator frequency	$\omega_r/2\pi$ (GHz)	6.752	6.308
Effective linewidth	κ_r (κ_f) $/2\pi$ (MHz)	0.427	0.294
Qubit-readout coupling	$g/2\pi$ (MHz)	46	54
Dispersive shift	$\chi/2\pi$ (MHz)	0.132	0.088
Relaxation time	$\overline{T}_1$ (μs)	30.6	83.8
Decoherence time	$\overline{T}_2^*$ (μs)	60.3	90.8
Qubit-coupler coupling	$g/2\pi$ (MHz)	47	64
Single-qubit gate fidelity	$\mathcal{F}_{1Q}$(%)	99.6%	99.8%

Table S1. **Measured qubit parameters, coherence properties, and single-qubit performance for the two qubits.** This pair of qubits is a subset of a larger 25-qubit device with similar performance.

* email: liangyuc@chalmers.se; email: jonas.bylander@chalmers.se; email: tancredi@chalmers.se